

## Observation of a Strong Infrared Magneto-Optical Effect in a Pyrite Type Ferromagnet $\text{CoS}_2$

Katsuaki SATO and Teruo TERANISHI

*Broadcasting Science Research Laboratories of Nippon Hoso Kyokai,  
1-10-11, Kinuta, Setagaya-ku, Tokyo 157*

(Received April 16, 1982)

Reflectance magneto-circular dichroism spectra and Kerr rotation spectra have been measured for the first time on a pyrite type ferromagnet  $\text{CoS}_2$ , for photon energies between 0.5 and 3.5 eV below the Curie temperature. There have been observed three major structures around 0.8, 1.5 and 2.8 eV, among which the most prominent is the one at 0.8 eV; the Kerr rotation reaches the value of  $1.1^\circ$  at the peak. Real and imaginary parts of the off-diagonal element of the dielectric tensor have been calculated from the observed spectra. Theoretical study has revealed that the line shape of the 0.8 eV structure can be explained in terms of the localized many-electron excitation associated with the  $d_x-d_y$  absorption edge of this compound. This corresponds to the narrow-band nature of the pyrite type compound.

### §1. Introduction

We have been working on optical studies of pyrite type compounds to get insight into the electronic structures of these materials and to clarify the effect of the electronic correlation in the pyrite system.

Among the pyrite type compounds  $\text{CoS}_2$  has been known as a metallic conductor with a ferromagnetic ordering below  $T_c$  ( $\sim 120$  K)<sup>1)</sup> and has been attracting much attention as a typical example for which the theory of the itinerant-electron magnetism has been successfully applied.<sup>2)</sup>

In our preceding paper on reflectivity and absorption spectra of  $\text{CoS}_2$  we reported that absorption bands due to interband transitions are located around 1.2 and 3.5 eV.<sup>3)</sup>

In order to get further information on the electronic structures related to these interband transitions magneto-optical spectra of this compound have been investigated. In this paper it will be shown that three major magneto-optical structures are observed at 0.8, 1.5 and 2.8 eV and that the structure at 0.8 eV can be interpreted in terms of the excitonic transition associated with the transition from the  $d_x$ -valence band to the  $d_y$ -conduction band.

The paper contains four major sections: In §2 are presented experimental techniques, in

§3 results, in §4 calculations of dielectric tensor elements and in §5 analysis of the magneto-optical line shapes and discussions.

### §2. Experimental Techniques

Single crystals of  $\text{CoS}_2$  were grown by the chemical transport method as described in the preceding paper.<sup>3)</sup>

Polar magneto-optical spectra were measured against one of the  $\{111\}$  natural surfaces of as-grown single crystals. The specimen was mounted on a copper-block sample holder attached to the variable-temperature insert of the cryostat for a superconducting magnet. Temperature was varied between 4.2 and 125 K. Magnetic field up to 8 kOe was applied perpendicular to the sample surface.

Spectra of the reflectance magneto-circular dichroism (hereafter it will be referred to as RMCD) and the Kerr rotation angle were measured by using a specially designed spectrometer employing a piezo-birefringent modulator. Details of the apparatus have been described elsewhere.<sup>4)</sup> Data were stored on a floppy disk file and processed by a micro-computer system. Further analysis such as to get the off-diagonal dielectric tensor elements has been performed by the aid of an IBM-370 computer.

It would be noted that the Kerr rotation measurement for the visible wavelengths was

very difficult due to superposition of the strong Faraday rotation introduced by the fused silica window of the cryostat. For infrared region such effect is negligible compared with the true Kerr rotation signal from the specimen. As regards RMCD, window effect was less serious even at short wavelengths.

### §3. Experimental Results

The RMCD is defined as the ratio of difference between reflectivities for RCP (right circularly polarized light) and LCP (left circularly polarized light) to the averaged reflectivity:

$$\Delta R/R = (R^+ - R^-) / \{(R^+ + R^-)/2\}, \quad (1)$$

where  $R^+$  and  $R^-$  denote the reflectivities for RCP and LCP, respectively.

The RMCD spectrum of  $\text{CoS}_2$  between 0.5 and 3.5 eV measured at 4.2 K under the magnetic field of 4 kOe is shown by a solid curve in Fig. 1. The reproducibility of the spectrum was checked by repeated measurements and by alternating samples. The resolution of the spectrum was 6 nm for  $350 \text{ nm} < \lambda < 900 \text{ nm}$ , 12 nm for  $900 \text{ nm} < \lambda < 1600 \text{ nm}$ , and 24 nm for  $1600 \text{ nm} < \lambda < 2500 \text{ nm}$ .

A prominent dispersive line shape has been observed around 0.8 eV (named A) as well as two broad structures around 1.5 eV (B) and 2.8 eV (C).

In Fig. 2 is given an observed Kerr rotation spectra of  $\text{CoS}_2$  at 4.2 K. Since it was difficult to separate the true rotation signal of the sample

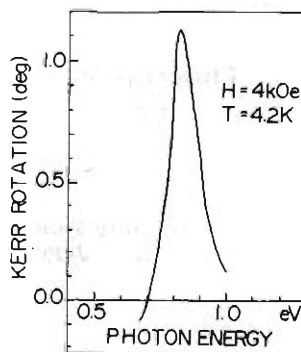


Fig. 2. Kerr rotation spectrum of a  $\text{CoS}_2$  single crystal at 4.2 K.

from the strong back-ground of the Faraday rotation of cryostat windows for photon energies above 1.0 eV, the spectrum is shown only for 0.5–1.0 eV. The Kerr rotation spectrum shows a peak at 0.82 eV where the rotation angle reaches a value of  $1.1^\circ$ . This value is relatively large compared with the one reported on other transition metal sulfides; e.g.  $0.22^\circ$  for  $\text{CdCr}_2\text{S}_4$ .

Figure 3 represents a magnetic field dependence of the peak-to-peak value of the dispersive line-shape of RMCD at 0.8 eV (structure A), from which we know that the sample is saturated magnetically by application of a magnetic field greater than 3 kOe. This result is consistent with the reported magnetization curve of  $\text{CoS}_2$ .<sup>5)</sup>

In Fig. 4 is shown a temperature variation of RMCD spectra around 0.8 eV. The peak-to-peak value of the A-structure decreases as the temperature is increased until it vanishes

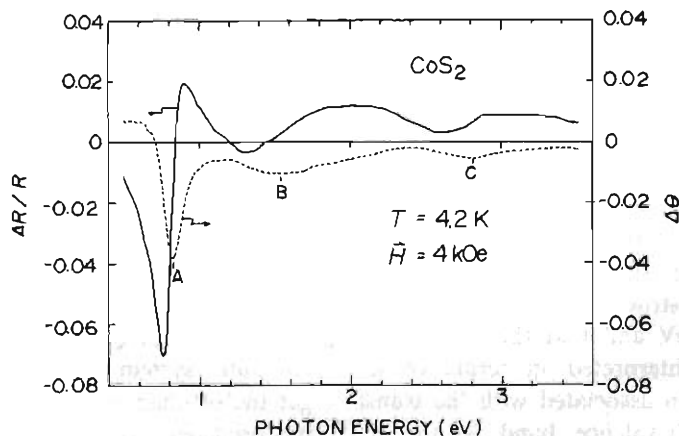


Fig. 1. Solid curve—A spectrum of RMCD ( $\Delta R/R$ ) of a  $\text{CoS}_2$  single crystal measured at 4.2 K under the magnetic field of 4 kOe. Dotted curve—A spectrum of  $\Delta\theta$  calculated from the RMCD spectrum by eq. (2).

above  $T_c$  (120 K) as shown by open circles in Fig. 5. Such a temperature dependence can be approximated by a magnetization curve predicted by the molecular-field theory as plotted by a dotted curve in Fig. 5. In addition, the

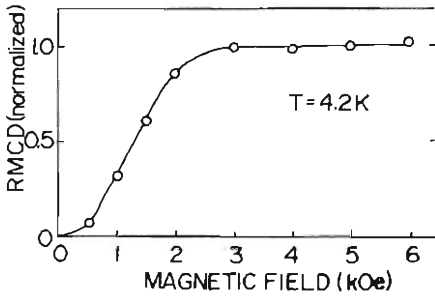


Fig. 3. Magnetic field dependence of the peak-to-peak value of the dispersive line shape of RMCD structure A. Data are normalized by the saturation value.

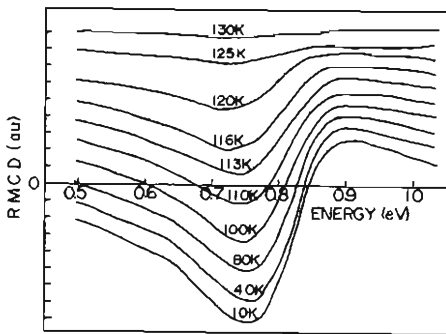


Fig. 4. Temperature variation of RMCD structure A under the magnetic field of 4 kOe. Zero level of each curve is shifted for the sake of clarity.

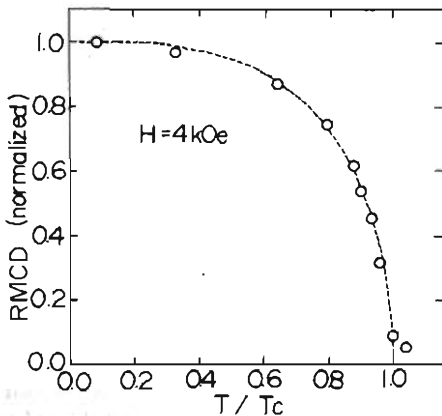


Fig. 5. Open circles—Temperature dependence of the peak-to-peak value of A-structure. Dotted curve—Temperature dependence of the magnetization expected by the molecular-field theory;  $S=1/2$  Brillouin function.

center frequency of the A-structure shows a slight shift ( $\sim 0.02$  eV) in the vicinity of the Curie temperature.

§4. Evaluation of Off-diagonal Dielectric Tensor Elements

From the obtained RMCD spectrum we calculate a spectrum of  $\Delta\theta$ , where  $\Delta\theta$  stands for a difference between phase shifts for RCP and LCP; i.e.  $\Delta\theta = \theta^+ - \theta^-$ . This parameter is one which is conjugate to RMCD  $\Delta R/R$ ,\* and can be evaluated from the RMCD spectrum by the following dispersion relation derived from the Kramers-Kronig relation by Smith.<sup>6)</sup>

$$\Delta\theta = \frac{1}{\pi} \mathcal{P} \int_0^\infty \frac{\omega' \Delta R/R(\omega')}{\omega'^2 - \omega^2} d\omega'. \quad (2)$$

Extrapolation parameters for the evaluation were so determined that the obtained  $\Delta\theta$  spectrum corresponds to the Kerr rotation spectrum shown in Fig. 2. The calculated  $\Delta\theta$ -spectrum is given by a dotted curve in Fig. 1. Phenomenologically the magneto-optical effect of an isotropic medium is described by a dielectric tensor,

$$\hat{\epsilon} = \begin{bmatrix} \epsilon_0 & -i\epsilon_1 & 0 \\ i\epsilon_1 & \epsilon_0 & 0 \\ 0 & 0 & \epsilon_z \end{bmatrix}, \quad (3)$$

where  $\epsilon_0 = \epsilon'_0 + i\epsilon''_0$  and  $\epsilon_1 = \epsilon'_1 + i\epsilon''_1$ . In our convention the electromagnetic wave is described by  $e^{-i\omega t}$ . It has been known that the off-diagonal elements give rise to the magneto-optical effect.

The real part  $\epsilon'_1$  and the imaginary part  $\epsilon''_1$  can be evaluated from  $\Delta R/R$  and  $\Delta\theta$  by following equations:<sup>10)</sup>

$$\begin{aligned} \epsilon'_1 &= -\frac{1}{4} \{ n(1 - n^2 + 3k^2)(\Delta R/R) \\ &\quad - 2k(1 - 3n^2 + k^2)\Delta\theta \}, \\ \epsilon''_1 &= -\frac{1}{4} \{ k(1 - 3n^2 + k^2)(\Delta R/R) \\ &\quad + 2n(1 - n^2 + 3k^2)\Delta\theta \}. \end{aligned} \quad (4)$$

Here  $n$  and  $k$  are the conventional optical constants which can be related to the diagonal element of (3), i.e.  $\epsilon_0 = \epsilon'_0 + i\epsilon''_0$  by equations

$$\epsilon'_0 = n^2 - k^2, \quad \epsilon''_0 = 2nk. \quad (5)$$

\* Simple relations between RMCD parameters and Kerr parameters can be easily derived as follows;  $\Delta\theta = -2\phi_K$  and  $\Delta R/R = 4\eta_K$ , where  $\phi_K$  represents the Kerr rotation and  $\eta_K$  the Kerr ellipticity.

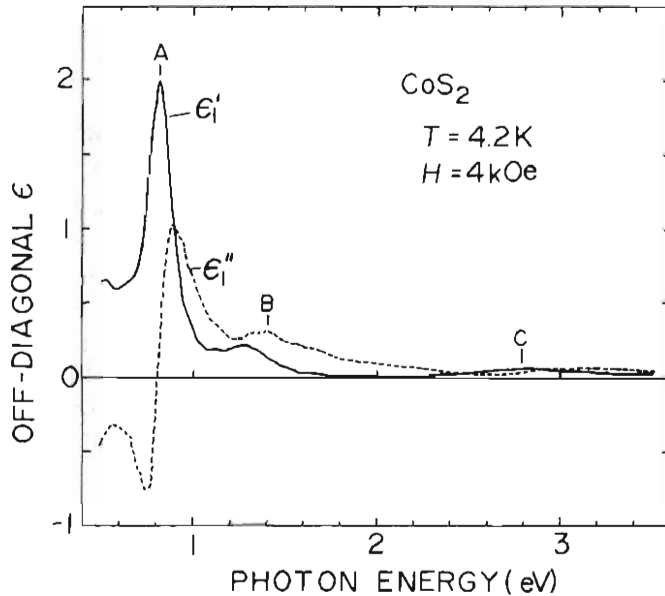


Fig. 6. Spectra of  $\epsilon_1'$  and  $\epsilon_1''$  calculated from the experimental data. Solid curve— $\epsilon_1'$ , Dotted curve— $\epsilon_1''$ .

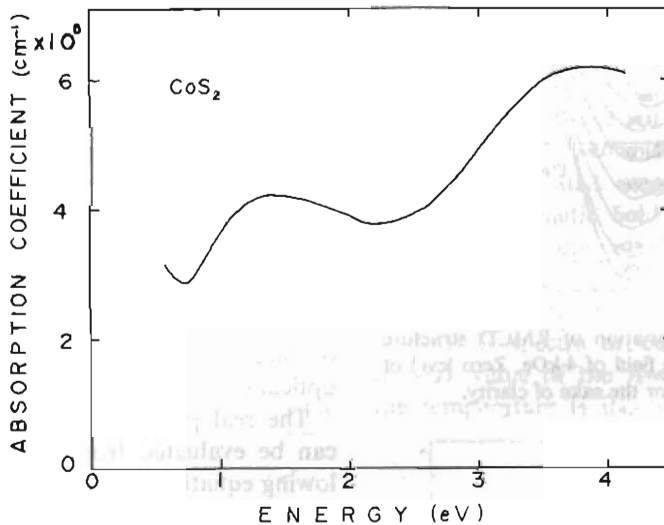


Fig. 7. Optical absorption spectrum of a  $\text{CoS}_2$  film.<sup>3)</sup>

In order to evaluate  $\epsilon_1'$  and  $\epsilon_1''$  by using eq. (4) we have employed room-temperature values of  $n$  and  $k$  reported in our preceding paper,<sup>3)</sup> since no 4.2 K-datum has been available. This is reasonable since only a slight variation in the reflectivity has been observed in our preliminary experiment down to 18 K. The calculated spectra of  $\epsilon_1'$  and  $\epsilon_1''$  are illustrated in Fig. 6.

In Fig. 6 one can observe a strong peak of  $\epsilon_1'$  at 0.8 eV and a weak peak at 1.4 eV as well as weak dispersive structure around 2.8 eV.

## §5. Discussion

In this section we give a theoretical analysis on the most prominent structure A observed at 0.8 eV. By referring to the absorption spectrum shown in Fig. 7,<sup>3)</sup> we know that this energy position falls on the one at which the lowest band-to-band absorption of this material starts.\* This absorption band has been tenta-

\* The absorption below 0.8 eV seen in Fig. 7 may be attributed to the intraband transition which obeys the Drude's law.

tively assigned to the transition from the filled  $d\epsilon$ -band to the empty portion of the  $d\gamma$ -band above the Fermi level.<sup>7)</sup> If this is the case a heavy hole left in the  $d\epsilon$ -orbital by the optical transition may bind an excited electron in the  $d\gamma$ -conduction band, producing an excitonic bound state. Such an excitonic transition may be approximated by the many-electron picture localized at Co atom;  $d\epsilon^6d\gamma \rightarrow d\epsilon^5d\gamma^2$ .

In the pyrite structure a Co atom is surrounded by a distorted octahedron of sulfur atoms and has a site-symmetry of  $C_{3i}$ . However, in the following discussions it will be treated as cubic symmetry for the sake of simplicity. Multiplets in the  $3d^7$ -low spin configuration in the octahedral symmetry can be described by the Sugano-Tanabe diagram;<sup>8)</sup> the ground multiplet is  ${}^2E$ , the lowest excited multiplet  ${}^4T_1$  and the next lowest  ${}^2T_1$  and  ${}^2T_2$ . The transition  ${}^2E \rightarrow {}^4T_1$  can be excluded since it is very weak due to its spin-forbidden nature. In the  ${}^2E \rightarrow {}^2T_1$  transition a majority spin is excited so that two  $d\gamma$ -electrons have parallel spins, whereas in the  ${}^2E \rightarrow {}^2T_2$  transition minority spin is excited making antiparallel spins in the  $d\gamma$ -band. The latter state can be thought to have higher energy than the former due to the electronic correlation. Therefore we assign the observed excitation to the transition  ${}^2E \rightarrow {}^2T_1$ .

Next, we evaluate an effect of the spin-orbit interaction on the  ${}^2T_1$  state. It can be shown by a simple calculation that the  ${}^2T_1$  state is split into a doubly degenerate  $\Gamma_6$  state and a quadruply degenerate  $\Gamma_8$  state with an energy separation of  $3\zeta/2$  as shown in Fig. 8. Here  $\zeta$  stands for the spin-orbit parameter of  $Co^{2+}$  ion. Eigenfunctions are as follows:

$$\begin{aligned}
 |\phi_1^\pm\rangle &= \frac{1}{\sqrt{2}} \left( \left| \alpha, \pm \frac{1}{2} \right\rangle \pm i \left| \beta, \pm \frac{1}{2} \right\rangle \right), \\
 |\phi_2^\pm\rangle &= \mp \frac{1}{\sqrt{6}} \left( \left| \alpha, \mp \frac{1}{2} \right\rangle \pm i \left| \beta, \mp \frac{1}{2} \right\rangle \right. \\
 &\quad \left. \mp 2 \left| \gamma, \mp \frac{1}{2} \right\rangle \right), \quad (6)
 \end{aligned}$$

for  $\Gamma_8$  ( $E = -\zeta/2$ ) and

$$\begin{aligned}
 |\phi_3^\pm\rangle &= \pm \frac{1}{\sqrt{2}} \left( \left| \alpha, \mp \frac{1}{2} \right\rangle \pm i \left| \beta, \mp \frac{1}{2} \right\rangle \right. \\
 &\quad \left. + \left| \gamma, \pm \frac{1}{2} \right\rangle \right), \quad (7)
 \end{aligned}$$

for  $\Gamma_6$  ( $E = \zeta$ ).

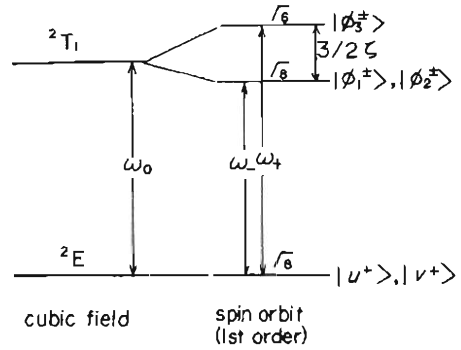


Fig. 8. An energy level scheme associated with the optical transition at 0.8 eV: Excited state is  ${}^2T_1$  which is split by the spin-orbit interaction in the first order. Ground state is  ${}^2E$ .

Here energy is measured from that of the unperturbed  ${}^2T_1$  state and  $|\alpha\rangle, |\beta\rangle$  and  $|\gamma\rangle$  denote the basis functions for the triply degenerate irreducible representation  ${}^2T_1$ .

On the other hand, the ground multiple  ${}^2E$  is not split by the first order spin-orbit interaction, but split by the exchange interaction into majority-spin and minority-spin states; the magnitude of the splitting can be estimated to be of the order of 0.01 eV from the temperature shift of the energy of the A-structure in the vicinity of the Curie temperature as stated in the previous section. Since the splitting is large enough compared with the temperature of measurements we can assume that only the states  $|u, +\frac{1}{2}\rangle$  and  $|v, +\frac{1}{2}\rangle$  are populated, where  $|u\rangle$  and  $|v\rangle$  represent basis function for the representation E.

As will be discussed later analysis of a magneto-optical line shape needs a knowledge of the transition matrix elements  $\bar{P}_{mn}^\pm$  for RCP(+) and LCP(-). We calculated  $\bar{P}_{mn}^\pm$  for transition between the ground state  ${}^2E$  and the excited state  ${}^2T_1$  and the results are summarized in Table I. In the table  $M = -(1/\sqrt{3})\langle te^2 {}^2T_1 || \bar{P}({}^2T_1) || e^3 {}^2E \rangle$  stands for the reduced matrix element between  ${}^2T_1$  and  ${}^2E$ .

According to Kohn and Kamimura<sup>9)</sup> the magneto-optical tensor element can be described as follows:

$$\begin{aligned}
 \epsilon_1 &= \epsilon'_1 + i\epsilon''_1 \\
 &= (2\pi N/\hbar) \sum_m \sum_n (f_m - f_n) \frac{\omega_{mn}^2}{\omega} \frac{1}{\omega_{mn}^2 - (\omega - i\Gamma)^2} \\
 &\quad \times \{ |\bar{P}_{mn}^+|^2 - |\bar{P}_{mn}^-|^2 \}. \quad (8)
 \end{aligned}$$

In this equation  $\hbar\omega_{mn}$  ( $= E_m - E_n$ ) means an

Table I. Transition matrix element between  ${}^2E$  and  ${}^2T_1$  for RCP and LCP.

$\bar{P}_{mn}^+$ (RCP)			
${}^2E \setminus {}^2T_1$	$ \phi_1^+\rangle$	$ \phi_2^+\rangle$	$ \phi_3^+\rangle$
$ \mu, 1/2\rangle$	0	$-1/\sqrt{6}$	$1/\sqrt{3}$
$ \nu, 1/2\rangle$	$\sqrt{3}/\sqrt{2}$	0	0
$\times M$			
$\bar{P}_{mn}^-$ (LCP)			
${}^2E \setminus {}^2T_1$	$ \phi_1^+\rangle$	$ \phi_2^+\rangle$	$ \phi_3^+\rangle$
$ \mu, 1/2\rangle$	$-1/\sqrt{2}$	0	0
$ \nu, 1/2\rangle$	0	$1/\sqrt{2}$	-1
$\times M$			

energy necessary to excite an electron from  $n$ -th ground state to the  $m$ -th excited state, and  $f_i$  ( $=\exp(-E_i/kT)/\sum_l \exp(-E_l/kT)$ ) an electron population in the  $i$ -th state; for sufficiently low temperatures  $f_m=0$  and  $f_n=1$  can be assumed. By applying the values listed in Table I to the matrix elements  $\bar{P}_{mn}^\pm$ , we get the following simple equations for  $\epsilon_1'$  and  $\epsilon_1''$ ;

$$\epsilon_1' = \frac{2\pi N}{\hbar} \left\{ \frac{\omega_-^2}{\omega} \frac{\omega_-^2 - \omega^2 + \Gamma^2}{(\omega_-^2 - \omega^2 + \Gamma^2)^2 + 4\omega^2\Gamma^2} - \frac{\omega_+^2}{\omega} \frac{\omega_+^2 - \omega^2 + \Gamma^2}{(\omega_+^2 - \omega^2 + \Gamma^2)^2 + 4\omega^2\Gamma^2} \right\} \frac{2}{3} M^2,$$

$$\epsilon_1'' = \frac{2\pi N}{\hbar} \left\{ \frac{2\omega_-^2\Gamma}{(\omega_-^2 - \omega^2 + \Gamma^2)^2 + 4\omega^2\Gamma^2} - \frac{2\omega_+^2\Gamma}{(\omega_+^2 - \omega^2 + \Gamma^2)^2 + 4\omega^2\Gamma^2} \right\} \frac{2}{3} M^2, \quad (9)$$

where  $\omega_+ = \omega_0 + \zeta$  and  $\omega_- = \omega_0 - \zeta/2$ ,  $\hbar\omega_0$  being the energy between the unperturbed excited state and the ground state.

Calculated spectra of  $\epsilon_1'$  and  $\epsilon_1''$  were com-

pared with the experimental data. The best fit was obtained with  $\zeta = 533 \text{ cm}^{-1}$ , a value of a free  $\text{Co}^{2+}$  ion and  $\Gamma = 1000 \text{ cm}^{-1}$ , a conventional line width value, as shown in Fig. 9. It becomes clear that a many-electron picture is valid to the optical transition in  $\text{CoS}_2$ , even though it has a metallic conduction property. This analysis also provides a strong evidence that the  $d\epsilon$ -state is involved in the 0.8 eV optical transition of  $\text{CoS}_2$ , since the spin-orbit interaction due to the  $d\epsilon$ -hole is essential to the large magneto-optical effect.

For other magneto-optical structures we have no definite explanation in this stage. Theoretical investigations especially of the energy band calculation will be helpful to further interpretation of the magneto-optical spectrum.

## §6. Conclusion

A strong magneto-optical effect has first been observed at 0.8 eV in a pyrite type ferromagnet  $\text{CoS}_2$ . The line shape is analyzed in terms of a localized many-electron excitation associated with the  $d\epsilon$ - $d\gamma$  interband transition of this material. Best fit of the calculated line shape to the experimental one has been obtained with reasonable parameters of the spin-orbit interaction and the line width. It turns out from this analysis that the correlation effect is essential in the  $d$ -band of the pyrite type compounds.

## Acknowledgement

The authors are very grateful to Professor H. Kamimura for continuous encouragement

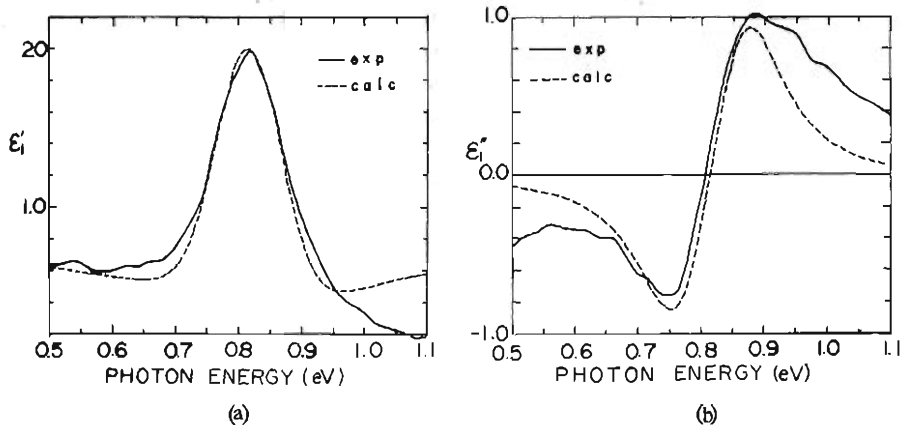


Fig. 9. Magneto-optical line shapes calculated by eq. (9), compared with the experimental curves. (a)  $\epsilon_1'$ ; base line for calculated curve is shifted to avoid the effect of other transition. (b)  $\epsilon_1''$ .

and invaluable discussions on this work. They are also indebted to Mr. K. Sakai for his help in the computer analysis of the magneto-optical line shapes.

### References

- 1) H. S. Jarrett, W. H. Cloud, R. J. Bouchard, S. R. Butler, C. G. Frederick and J. L. Gillson: *Phys. Rev. Lett.* **21** (1968) 617.
  - 2) T. Moriya: *J. Magn. & Magn. Mater.* **14** (1979) 1.
  - 3) K. Sato and T. Teranishi: *J. Phys. Soc. Jpn.* **50** (1981) 2069.
  - 4) K. Sato: *Jpn. J. Appl. Phys.* **20** (1981) 2403.
  - 5) V. Johnson and A. Wold: *J. Solid State Chem.* **2** (1970) 209.
  - 6) D. Y. Smith: *J. Opt. Soc. Amer.* **66** (1976) 547.
  - 7) T. A. Bither, R. J. Bouchard, W. H. Cloud, P. C. Donohue and W. J. Siemens: *Inorg. Chem.* **7** (1968) 2208.
  - 8) S. Sugano, Y. Tanabe and H. Kamimura: *Multiplets of Transition-Metal Ions in Crystals* (Academic Press, New York, 1970).
  - 9) K. Kohn and H. Kamimura: *Jiseitai Handbook* (Asakura-shoten, Tokyo, 1975) Chap. 19, p. 1011 [in Japanese].
  - 10) K. Sato: *J. Phys. Soc. Jpn.* **43** (1977) 719.
-